Exp Brain Res (2006) 171: 116–128
DOI 10.1007/s00221-005-0252-2

RESEARCH ARTICLE

Martha Flanders · Leigh A. Mrotek · C.C.A.M. Gielen

Planning and drawing complex shapes

Received: 15 March 2005 / Accepted: 11 October 2005 / Published online: 25 November 2005
© Springer-Verlag 2005

Abstract Arm and hand movements are generally controlled using a combination of sensory-based and memory-based guidance mechanisms. This study examined similarities and differences in visually-guided and memory-guided arm movements, and sought to determine as to what extent certain control principles apply to each type of movement. In particular, the 2/3 power law is a principle that appears to govern the formation of complex, curved hand trajectories; it specifies that the tangential velocity should be proportional to the radius of curvature raised to an exponent of 1/3. A virtual reality system was used to project complex target paths in three-dimensional (3D) space. Human subjects first tracked (with the tip of a handheld pen) a single target moving along an unseen path. The entire target path then became visible and the subject traced the shape. Finally, the target shape disappeared and the subject was to draw it, in the same 3D space, from memory. Most aspects of the movements (speed, path size, shape and arm postures) were very similar across the three conditions. However, subjects adhered to the 2/3 power law most closely in the tracing condition, when the entire target path was visible. Also, only within the tracing condition, there were significant differences in the value of the exponent depending on the size and the spatial orientation of the trajectory. In the tracking and drawing conditions, the exponent was greater than 1/3, indicating that subjects spent more time in areas of tight curvature. This may represent a strategy for learning and remembering the complex shape.

M. Flanders (✉) · L. A. Mrotek
Department of Neuroscience, University of Minnesota,
6-145 Jackson Hall, 312 Church St. S.E.,
Minneapolis, MN 55455, USA
E-mail: fland001@umn.edu
Tel.: +612-624-6601
Fax: +612-626-5009

C.C.A.M. Gielen
Department of Medical Physics and Biophysics,
Radboud University Nijmegen, Nijmegen, The Netherlands

Keywords Learning · Hand tracking · Arm movement · Trajectory formation · Two-thirds power law · Drawing from memory

Introduction

Imagine carving a sculpture in wet clay. You directly observe the model's silhouette and copy it into your sculpture, but, at times, you ignore the model and work from memory. You also guide your knife to visible rough spots for further refinement. Routine tasks such as shaving, shaping the hand around an object, and making an expressive gesture, involve a similar hybrid of sensory and internal guidance. In fact, although these two mechanisms have provided a useful dichotomy for studies of sensorimotor systems, most of our arm and hand movements seamlessly combine aspects of sensory-based and memory-based control.

Thus, we sought to tease apart aspects of arm movement that may or may not differ across a range of sensory-based and memory-based conditions. We compared a number of movement characteristics across the following conditions: (1) tracking a target that moves with a particular time course, along an unseen path, (2) self-paced tracing of the same path, now entirely visible as the outline of a three-dimensional (3D) shape, and (3) self-paced drawing of the again invisible shape, from memory.

In the companion paper (Mrotek et al. 2005), we examined, in detail, our results from the tracking condition. As the target made four consecutive cycles around a closed shape, tracking improved to steady state about three-fifths of the way through the first cycle. Steady-state tracking exhibited evidence of anticipation, suggesting that subjects had "learned" something about the target trajectory. Furthermore, compared to the subsequent tracing condition (where the target path was entirely visible), during tracking, the hand path was spatially distorted: it was flatted into the frontal plane due to relatively poor tracking in depth.

We wondered if we would also find consistent spatial distortions when we compared tracing the visible shape to drawing that shape from memory. This was motivated by a broad literature on memory versus visual guidance (e.g., Gnadt et al. 1991) as well as specific examples from studies of reaching to remembered target points in 3D (e.g., McIntyre et al. 1997, 1998). In one of the first such studies, Soechting et al. (1990) found that finger placement was centered around the eyes when the finger was visible, but around the shoulder when it was not. Thus, in the present study, we hypothesized that subjects might distort the remembered shape by centering it around the eyes or the shoulder. Other distortions are also possible, such as rotating and flattening the remembered shape into the frontal plane (Klein Breteler et al. 2003).

Along these same lines, we wondered if the target shape would be properly remembered and executed as containing planar segments, or alternatively, if the tendency for piecewise planar segments (Soechting and Terzuolo 1987) might be enhanced or degraded in memory. We also sought to test the idea that after the extensive practice of the tracking and tracing conditions, the planning of joint angle trajectories might be improved to allow the memory-guided movements be generated in a more energetically efficient style (Klein Breteler et al. 2003; Flanders et al. 2003). Thus we computed kinetic energy in each trial and compared it across conditions.

Finally, we aimed to compare the adherence of the subjects to the 2/3 power law (Lacquaniti et al. 1983) across the three conditions of our study (tracking, tracing and drawing). This law prescribes a nonlinear relationship between the tangential velocity and the radius of curvature of the hand trajectory; if the power law is written as $v(t) = C\, r(t)^{b}$, the theoretical relation predicts an exponent of $b = 1/3$. Although there is a great deal of evidence for this phenomenon, its validity as a fundamental constraint of neural control has recently been questioned (Schaal and Sternad 2001; Richardson and Flash 2001). In a study where subjects drew planar ellipses with eyes closed, Schaal and Sternad (2001) reported systematic differences in the value of the power law exponent related to the size of the drawing and the plane of the movement (horizontal vs. vertical). The various studies on this topic have used many different sensory and mechanical conditions, including 2D, 3D, and even isometric conditions (Massey et al. 1992; Todorov and Jordan 1998), but few have compared the strategy of subjects across conditions. Thus, our goal was to use the exponent of the power relation to measure and interpret changes in trajectory formation across visual-memory conditions, and also within a condition, across shapes and across particular segments of a shape. For example, based on the work of Schaal and Sternad (2001), within the drawing condition we expected differences between shapes with different sizes, and differences between the horizontal and vertical segments of the same shape. Thus, the main aims of our study were to compare visually-guided and memory-guided drawings of a 3D trajectory, and to examine the validity of the 2/3 power law for various conditions of tracking, self-paced tracing and drawing from memory.

Methods

Subjects

The experimental procedures followed the human subjects regulations of Radboud University Nijmegen, where six subjects took part in the experiment. All subjects were neurologically normal and had normal or corrected to normal vision. The average age was 33 ± 12(SD) years, four of the subjects were female, and two of them were left-handed but performed with the right arm. (This was due to limitations of the experimental setup and we found no consistent differences between the right- and left-handed subjects.) In a preliminary attempt to study the influence of prior experience, we choose subjects with a wide range of familiarity with the target shapes: one subject had designed and tested the shapes, two were coauthors, and three were completely naïve about the shapes and the purpose of the experiment. Also, one of the experienced subjects and one of the naïve subjects performed the experiment twice. We did not find any evidence of an influence on account of prior experience, and for these two subjects, corresponding data from the two sessions were averaged. Thus, our data set was derived from $n = 6$ subjects.

Target conditions and target shapes

In each experimental session, each of the 17 target shapes was used once, in an order that was varied randomly across sessions. As shown in Fig. 1, targets were displayed in the 3D workspace directly in front of the seated subject, using a virtual reality system with an LCD projector and red/green glasses (Mrotek et al. 2005). As also indicated in Fig. 1, the data were measured and analyzed in a right-handed Cartesian coordinate system, with the Z-axis in the upward direction, the X-axis in the horizontal direction (to the subject's right), and the Y-axis in depth (orthogonal to the frontal plane of the subject's body).

The subject was first asked to track the center of a single target (a sphere with a diameter of 2.5 cm) moving along the perimeter of the unseen shape. After a rest (with the arm at the side) of about 30 s, the subject then traced the perimeter of the shape while it was entirely visible. Finally, the shape disappeared and after another 30 s rest period, the subject was asked to draw it, in the same 3D space, from memory. For the drawing condition, the target sphere appeared and remained at the initial position to help the subject begin the drawing in the correct location.

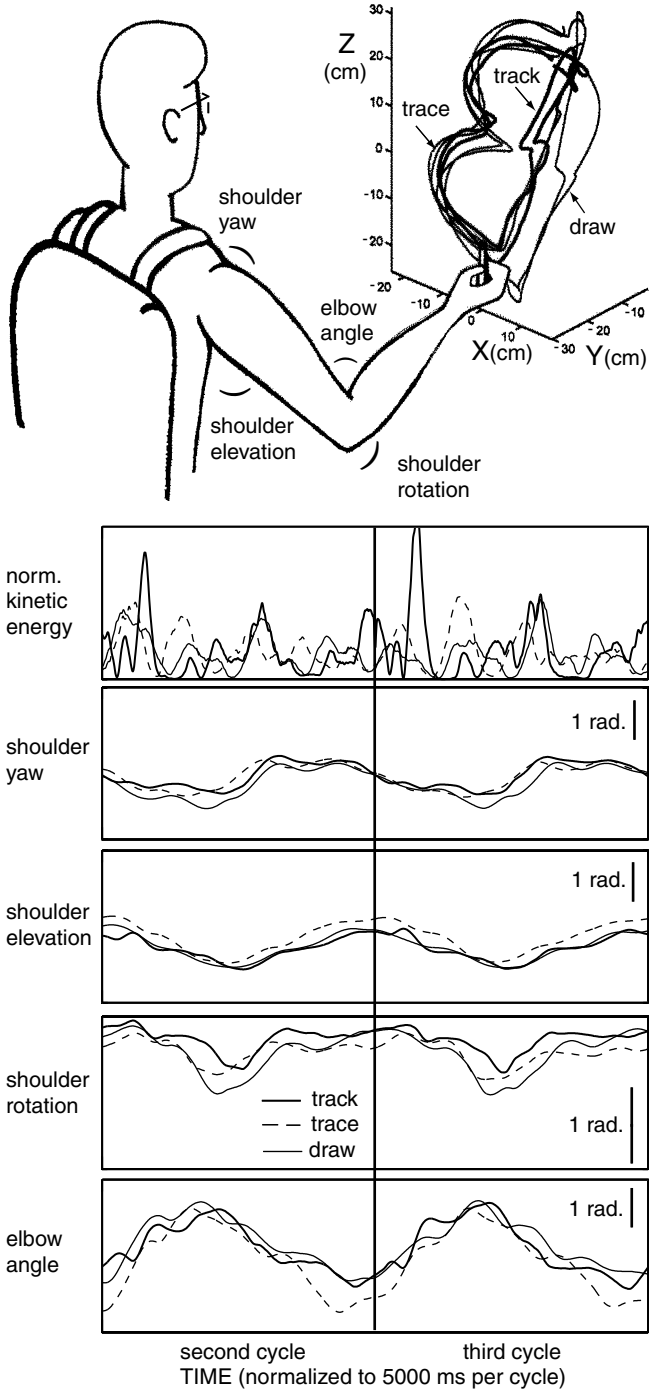

Fig. 1 Experimental setup and comparison across conditions. Hand paths (*top illustration*), normalized kinetic energy (*upper panel*) and joint angles (*lower panels*) are shown for the second and third cycles, for the three different conditions: tracking (*thick solid line*), tracing (*dashed line*) and drawing from memory (*thin solid line*), for the front 60° long axis bend Cassini shape. The subject wore red/green glasses for a three-dimensional view of the target, and tracked, traced, or drew from memory with the tip of a handheld pen. Movements were made in the clockwise direction. Kinetic energy (KE) showed more rapid fluctuations in the tracking condition. However, the average KE across the two cycles was similar in all conditions. Also, joint angles were similar across conditions

For the tracking trials, the target moved around the shape four times, with a speed profile that approximated the 2/3 power law (Mrotek et al. 2005). In the tracing and drawing conditions, subjects were instructed to "use the same speed" as in the tracking condition, and to complete four consecutive cycles. The experimenter (and not the subject) counted cycles silently and gave a verbal warning at the end of the third cycle, as well as an indication to stop at the end of the fourth cycle. As explained below, all analyses were applied only to data from the second and third cycles.

Target shapes are described in detail in the companion paper (Mrotek et al. 2005). Briefly, the main shape was a Cassini ellipse, presented either in a front or a side orientation (Fig. 2, top row). The long axis was 48 cm and the width was 32 cm. For both the front and the side orientations, we produced variations of the Cassini shape by folding it at an angle of either 30° or 60°. These folds were either down the long axis (Fig. 2, bottom right panel), across the short axis, or along an oblique axis (see Figs. 1–2 of Mrotek et al. 2005). This produced 14 of the 17 shapes. For Cassini shapes, in the tracking condition, each cycle took 5 s.

We also presented a more spherical shape, which we will refer to as the 4-plane shape, where four connected semicircles lay in horizontal and vertical planes (Fig. 2, bottom left panel). We presented three sizes of the 4-plane shape: the small shape was 16 cm in the frontal plane and 16 cm in depth (radius of the semicircles = 8 cm), the medium shape was 28×28 cm, and the large shape was 40×40 cm. In accord with the 2/3 power law, both the speed and the radius of curvature were constant. In the tracking condition, the target moved at a different constant speed for each size, such that each cycle took 6.7 s.

In Fig. 2, the Cassini shapes are shown from the perspective of the subject. The subject sat 90 cm from the large vertical screen (wearing the red/green glasses) and the height of the chair was adjusted so that the center of the shape was at the eye level (see Fig. 1). The projection of the 4-plane shape on the frontal plane was a square. Therefore, to give a better 3D view of the 4-plane shape, in Fig. 2 it is rendered as viewed from a position slightly to the right and above the eyes of the subject.

Data collection and processing

We used an Optotrak 3020 system (Northern Digital Inc., 100 Hz, precision better than 0.15 mm) to record the locations of LED markers, in three dimensions. The markers were placed on the right shoulder, elbow, and wrist, and on the tip of a pen-like object held in the subject's right hand ("hand marker"). Subjects were asked to refrain from bending the wrist, and thus they were to produce (track, trace or draw) the shape with the

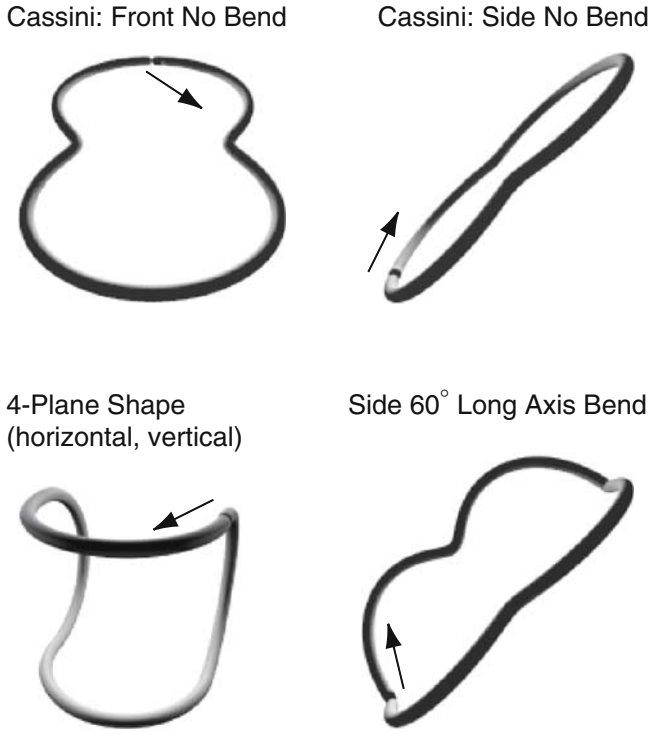

Fig. 2 Three-dimensional renderings of four of the 17 target shapes. The main shape used in this experiment was a peanut-shaped Cassini ellipse. It was presented in frontal view in a plane rotated 45° about the horizontal (*X*) axis, such that the bottom of the shape was closer to the subject (*upper left*), and in side view (*upper right*) where we rotated the shape 80° about the vertical (*z*) axis. In addition to these shapes, we altered the Cassini ellipse by folding it along three axes. It could be bent along the long axis (*lower right*), the short axis (not shown) or an oblique axis (not shown). The magnitude of the bends could be 60° (*lower right*) or 30° (not shown). For all Cassini shapes, the subject began at the location of the discontinuity and moved clockwise around the shape. All Cassini shapes are shown from the perspective of the subject. The other shape was a 4-plane shape, which consisted of four semicircles in horizontal and vertical planes (*lower left*). The subject began at the location of the discontinuity and moved as indicated by the *arrow*. The 4-plane shape is shown from a perspective to the right of and slightly above the subject's line of sight

hand marker, using mainly shoulder and elbow rotations. This allowed us to ignore the wrist and finger joints in the calculation of kinetic energy. Forearm pronation/supination was also allowed.

To avoid the transients associated with starting (at the beginning of the first cycle) and stopping (at the end of the fourth cycle), we focused the analysis on the second and third cycles. In the tracking condition, each target cycle had a fixed duration: 5 s for the Cassini shapes and 6.7 s for the 4-plane shapes. For tracing and drawing, the exact time cyle could vary. Therefore, for all conditions, we marked and extracted data from the center two cycles based on the distance of the hand marker from the starting target location. Using custom software, we found the minima of the distance versus time plot and extracted data (the *X*-, *Y*-, *Z*-locations of all markers) from the center two cycles.

Computing normalized kinetic energy

If the hand trajectory is similar across conditions, it is still possible that the hand followed this trajectory using sets of joint rotations that differed across conditions. For example, subjects may have used more elevated elbow locations during tracking, but a relatively low elbow location during drawing, and this would change the inertial resistance to joint rotations and therefore the kinetic energy (KE). A robust measure of slight changes in the arm configuration across similar movements is provided by a calculation of normalized KE. As described below, computing the average KE for each trial, while also taking into account the speed and distance, allowed us to summarize energetic efficiency with a single value for each subject in each condition.

We performed this calculation as described previously (Flanders et al. 2003), using three degrees of freedom at the shoulder and one at the elbow. This technique ignores shoulder translation and forearm pronation/supination, but is very sensitive to changes in the shoulder angles and the sequencing of the various joint rotations across time. The basic formula for kinetic energy is

$$\mathrm{KE} = 1/2\, mv^2 + 1/2\, I\Omega^2, \quad (1)$$

where m is the mass of the arm, v is the velocity of the center of mass, Ω is the joint angular velocity vector and I is the inertia tensor of the two-link arm. Obviously, a comparison of this parameter across conditions would be heavily influenced by slight changes in velocity. Therefore, to isolate the aspect of KE due to arm geometry and the sequencing of joint rotations, we applied the calculation to the center two cycles after each had been time-normalized to 5 s. We then computed the average normalized KE across each cycle and averaged the values for the two cycles to give one normalized KE value for each trial.

The amount of KE during each movement is also heavily influenced by the total distance of the hand path (i.e., the size of the shape), which may vary across conditions and across subjects. Therefore, to better isolate the aspect of KE due to arm configuration, and to combine normalized KE values across subjects, we used linear regression to relate this parameter to path distance (see Fig. 6d). For each condition and subject, we then evaluated this relation to find the predicted normalized KE value at a common distance (the average path distance across all subjects and conditions).

Planarity and 2/3 power law

Measures of hand path planarity and adherence to the 2/3 power law were applied to sub-cycles within the center two cycles. As illustrated in Figs. 3, 4, we used the minima of the hand speed profile to delineate sub-cycles. The hand paths for the two cycles along the 4-plane

shapes were divided into eight sub-cycles, corresponding to horizontal and vertical sections (Fig. 3). The two cycles along the Cassini shapes were divided into five to eight sub-cycles by virtue of the fact that the hand slowed down at bends (i.e., the locations of the 30° or 60° folds) and indents (the areas of tight curvature in between the two main lobes) (Fig. 4).

Deviation from planarity was measured as the SD of hand distances perpendicular to a plane that was fit to the 3D hand locations. For this analysis, we used a spatially balanced set of complete sub-cycles of the Cassini shapes: two for the no bend and short axis bend shapes (i.e., the full top and bottom lobes), and four for the shapes bent around long and oblique axes. For example, Fig. 4 shows data from the tracing of the side 60° long axis bend shape. The first segment (brown) was excluded and the next four segments (pink, purple, blue, green) were used, to give a balanced coverage of the shape.

Adherence to the 2/3 power law was evaluated using the slope of a linear regression fit to the relation between log hand velocity and log hand path radius of curvature. This gave us a separate slope value for each analyzed segment. For 4-plane shapes we used all eight sub-cycles (see Fig. 3). This gave four values for horizontal segments and four values for vertical segments, for each trial. For Cassini shapes, we excluded the first sub-cycle and used the next four sub-cycles (see Fig. 4), to yield an equal number of values for each shape. The value of the slope of log velocity versus log radius was then interpreted as described below.

Interpreting deviations from the 2/3 power law

We did a computer simulation to help explain our results. In this section, we will show that the 2/3 power law (Lacquaniti et al. 1983), which states that the radius $r(t)$ and velocity $v(t)$ are related by $r(t)/v(t) = C\, r(t)^{2/3}$ or in equivalent notation $v(t) = C\ r(t)^{1/3}$, follows in a straightforward way for a simple model, in which an object moves along a trajectory that is described by two orthogonal sinusoids (Hollerbach 1980). We will use this as a starting point to interpret deviations from the expected 0.33 value for the exponent.

The position of an object, that moves along a trajectory of two orthogonal sinusoids, 90° out of phase, is given by the elliptic trajectory

$$\begin{pmatrix} x(t) = A_x \cos(\omega t) \\ y(t) = A_y \sin(\omega t) \end{pmatrix}. \tag{2}$$

According to straightforward mathematics, the curvature $\kappa(t)$ of the ellipse at time t is given by

$$\kappa(t) = \frac{((\mathrm{d}x/\mathrm{d}t)(\mathrm{d}^2y/\mathrm{d}t2) - (\mathrm{d}y/\mathrm{d}t)(\mathrm{d}^2x/\mathrm{d}t^2))}{((\mathrm{d}x/\mathrm{d}t)^2 + (\mathrm{d}y/\mathrm{d}t)^2)^{3/2}}, \tag{3}$$

where $\mathrm{d}x/\mathrm{d}t$ and $\mathrm{d}^2x/\mathrm{d}t^2$ represent the first derivative (velocity) and second derivative (acceleration) of $x(t)$, respectively. More detailed information about Eq. 3 can be found in Stoker (1969). The curvature κ of this ellipse is equal to the inverse of the radius r of the path ($=1/r$).

Substitution of the first and second derivates of $x(t)$ and $y(t)$ in Eq. 2 gives

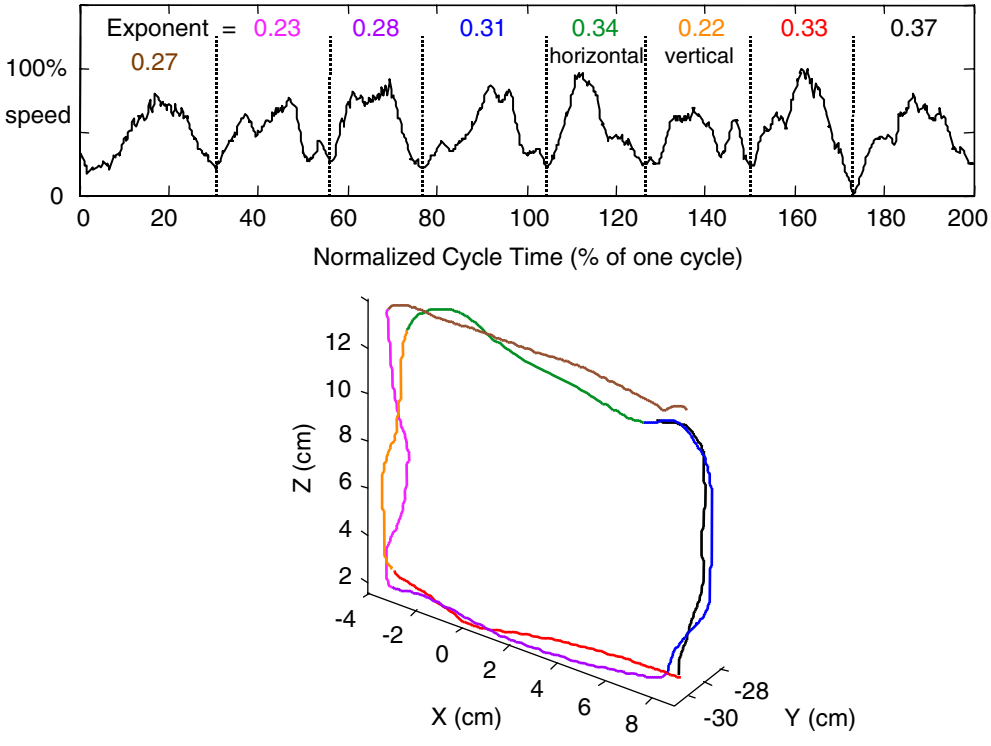

Fig. 3 Position (*lower panel*) and normalized tangential velocity (*upper panel*) are shown while the subject traced the small 4-plane shape. The hand paths for the two cycles along the 4-plane shape were divided into eight sub-cycles, indicated by different colors. The *vertical dotted lines in upper panel* indicate velocity minima. These occurred when the subject switched from a horizontal to a vertical plane or the other way around. Also shown, for each sub-cycle, is the value of the slope of log velocity versus log radius of curvature

$$\frac{1}{r(t)} = \kappa(t) = \frac{A_x A_y \omega^3 \sin^2(\omega t) + A_x A_y \omega^3 \cos^2(\omega t)}{v(t)^3} = \frac{\omega^3 A_x A_y}{v(t)^3}. \quad (4)$$

For constant amplitudes A_x and A_y and for constant frequency ω, we obtain $r(t) = \text{constant}\ v(t)^3$, or $\log v(t) = C + 1/3 \log r$.

According to the derivations above, we expect a slope of 0.33 if we plot log v(t) as a function of log r(t) for the simple model above. This is shown schematically in Fig. 5 (solid lines). The upper left panel shows the X- and Y-trajectories as a function of time (for 2.5 s). The upper right panel shows the elliptical path in the X-Y plane (for 5.0 s). The lower left panel shows the tangential velocity as a function of time (2.5 s) and the lower right panel shows the relation between log velocity and log radius, which follows a perfectly straight line with slope of 0.33.

Since several studies have reported exponents that deviate from the 0.33 value, we speculated about explanations for this behavior. One possible explanation might be that in various phases, the subjects move faster or slower than predicted by the simple model described above. Therefore, we did simulations to produce a model where the hand moves faster (slower) along relatively flat parts of the path, and slower (faster) along the tight-curvature parts of the path. For this purpose the model was modified into

$$\begin{pmatrix} x(t) = A_x \cos(\omega(t)t) \\ y(t) = A_y \sin(\omega(t)t) \end{pmatrix}, \quad (5)$$

where the angular velocity is not constant but instead depends on the phase of the elliptic trajectory.

The results are shown in Fig. 5 (dashed and dotted lines). The heavy dashed lines show the predictions for a model which moves faster in the relatively flat (large radius of curvature) areas and slower in the tight-curvature (small radius) areas. The dotted lines show the results for the opposite case: lower tangential velocity for flat sections and higher tangential velocity for tight curves. All trajectories in the X–Y plane (upper right panel) superimpose, but they differ in their velocity traces (lower left panel), and the slopes of the log velocity/log radius plots are clearly different. This simulation shows that a higher slope in the log v/log r plot is compatible with the idea that movement is faster than the simple model for a large radius of curvature (a gradual curve) and slower at a small radius of curvature (a tight curve, as occurs around an indent or at a bend).

Results

Similarity in geometry and average speed across conditions

Since the target was not visible in the drawing condition, we hypothesized that there might be a consistent spatial

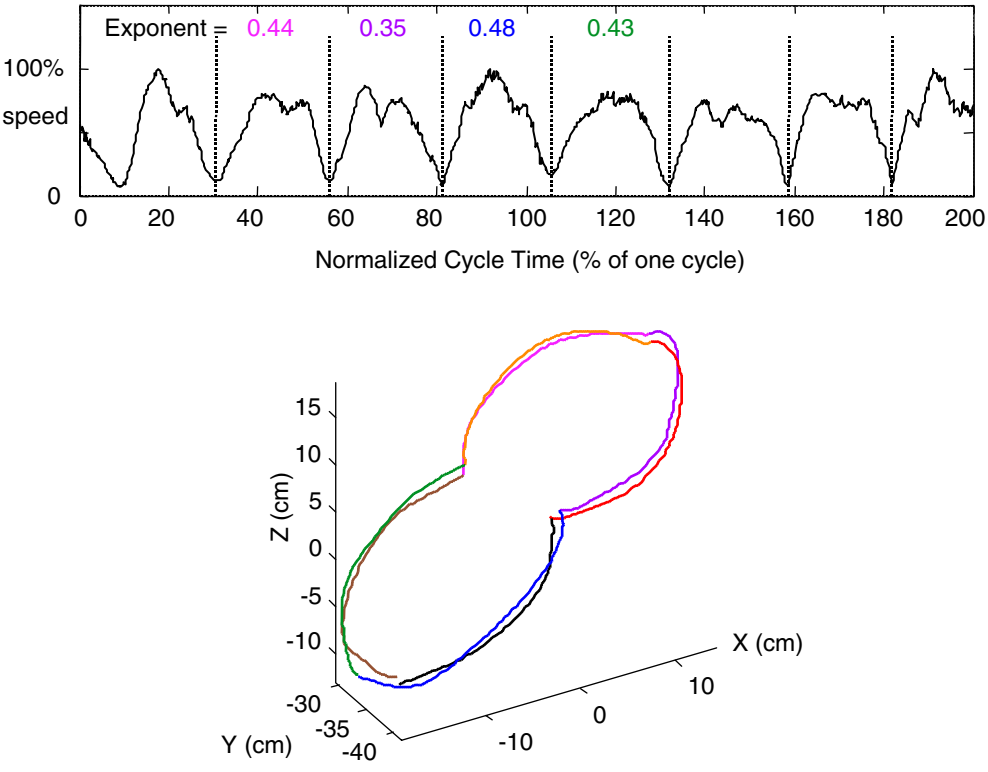

Fig. 4 Position (*lower panel*) and normalized tangential velocity (*upper panel*) for the side 60° long axis bend Cassini shape in the tracing condition. This subject produced a shape that was flatter than the 60° folded target shape, but other subjects followed the target more faithfully. The two cycles were divided into eight sub-cycles by virtue of the fact that the hand slowed down at bends (i.e., the locations of the 60° folds) and indents (the areas of tight curvature in between the two main lobes). The eight sub-cycles are shown in different colors. Sub-cycles 2–5 were used for the analysis of planarity and the 2/3 power law; the values of the slope of log velocity versus log radius of curvature are shown for these sub-cycles

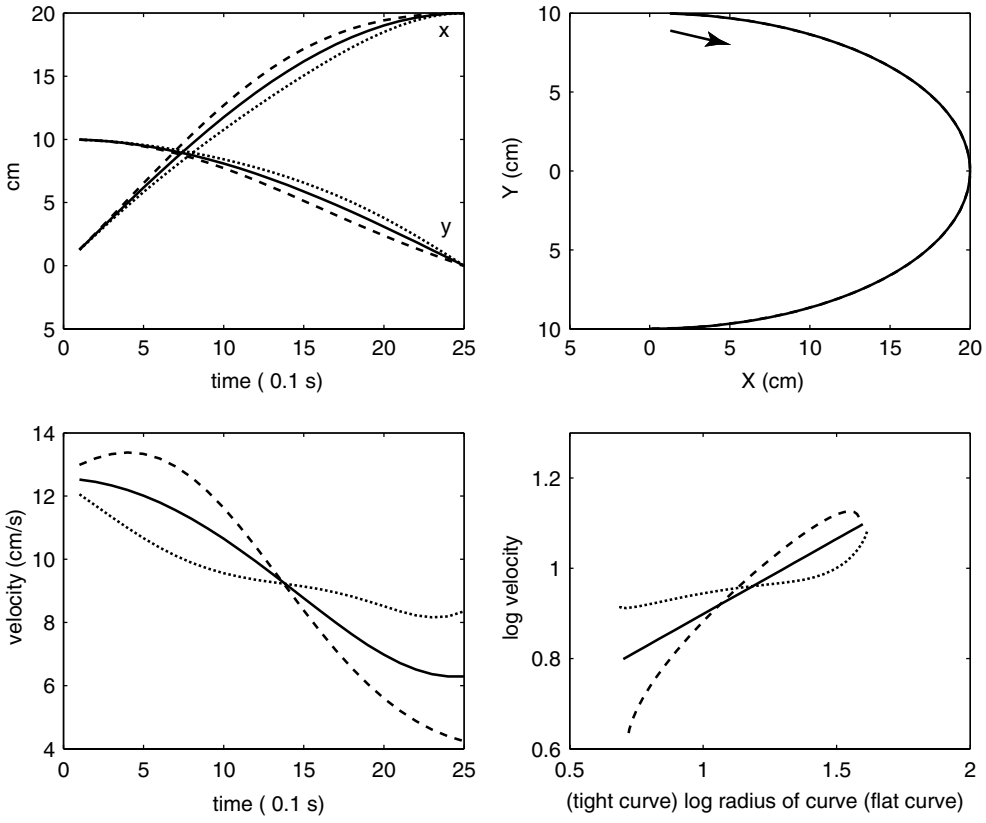

Fig. 5 Simulation to aid in understanding deviations from the 2/3 power law. *Solid black lines* represent a sinusoidal speed profile in both the *X*- and the *Y*-dimensions. The *X*- and *Y*-position values are plotted across time for 2.5 s (*top left panel*) along with the corresponding tangential velocity plot for 2.5 s (*bottom left panel*) and the elliptical hand path for 5.0 s (*top right panel*). For sinusoidal motion, log velocity versus log radius of curvature gives a slope of 0.33 (*bottom right panel*). In all panels, *dashed and dotted lines* represent deviations from the 0.33 slope (i.e., deviations from the value dictated by the 2/3 power law). A larger slope (*dashed lines*) represents a case where the hand moves more slowly during tight curves and more quickly along more gradual curves. A smaller slope (*dotted lines*) represents the opposite tendency

distortion in 3D shapes drawn from memory. As a first step in the analysis to test this hypothesis, we superimposed the pen-tip paths from the three conditions and rotated the plots to look for similarities and differences for each subject and for each shape. An example is shown in Fig. 1, where we have plotted the hand paths (top) and the joint angles (bottom) for the second and third cycles of the front 60° long axis bend shape. The tracking, tracing and drawing conditions are plotted with different line styles. The qualitative examination of all trials led to the conclusion that, although the six subjects exhibited small idiosyncratic spatial distortions in the memory condition, there was no common pattern.

Due to these qualitative observations, we did not attempt to quantify spatial rotations, translations or distortions in aspect ratios. However, we did fully quantify several other kinematic and kinetic parameters (Fig. 6). The results in Fig. 6 include all Cassini shapes (but not the 4-plane shapes) and show grand means across the six subjects and standard errors. The small and large 4-plane figures had path distances outside the range of the Cassini shapes, and all 4-plane shapes had tracking cycle periods that were different from those of the Cassini shapes (6.7 s instead of 5 s). Thus, to allow for linear regression and ANOVA tests on the pooled data, for this analysis, we chose to exclude the 4-plane shapes.

In spite of our instructions to use the same speed, some subjects traced and drew the shapes faster than the speed of the target in the tracking condition. Thus, the average cycle period was less than 5,000 ms for tracing and drawing (Fig. 6a). However, the difference across the three conditions was not statistically significant (ANOVA, $P > 0.05$). As expected, the standard error (across subjects) was very small in the tracking condition (black bar), but it was much larger in the tracing condition (white bar) and the drawing condition (gray bar). When six separate ANOVAs were applied, each of the six subjects showed a significant difference across conditions ($P < 0.001$). However, Scheffé post hoc analysis ($P < 0.05$) revealed several different trends for cycle period: for three subjects, the trend was track > trace = draw, for one subject, track > trace > draw; for one subject, track = trace > draw; and for the remaining subject, track < trace but the other conditions were not significantly different. Thus, the different subjects had different speed trends.

The overall size of the shape (path distance for each cycle) was not significantly different across conditions (Fig. 6b). However, due to the separate target calibrations (Mrotek et al. 2005) there was some variability across subjects in average size of all shapes, giving rise to the large error bars on the grand means. When a separate ANOVA was applied to each of the six subjects, the size was never significantly different across the conditions ($P > 0.05$). Apparently the flattening of the shape in the tracking condition (Mrotek et al. 2005) was offset by a tendency for manual tracking to deviate from the target path.

In Fig. 6c we show the results of our analysis of the geometry of the hand path during sub-cycles of all Cas-

sini shapes. As explained in Methods, cycles two and three were divided into sub-cycles by virtue of the fact that the hand trajectory slowed at indents and bends (see Fig. 4). For complete sub-cycles, we calculated the standard deviation of a 3D planar fit to the hand path data. The deviation from planarity was greater in the tracking condition compared to the tracing condition (ANOVA with Scheffé post hoc analysis, $P < 0.05$), but the drawing condition was not different from the other conditions. Thus, despite the possibility of inherent variability and distortion in the memory-guided condition (see Fig. 1), the deviation from planarity was not significantly greater than in the visually-guided movements.

Similarity in normalized kinetic energy across conditions

Normalized kinetic energy (nKE) also did not vary significantly across conditions (Fig. 6d, e), indicating that arm configuration and sequences of joint rotations remained constant. For example, in Fig. 1 we show, for the center two cycles of the front 60° long axis bend shape, the similarity in one subject's joint rotations across the three conditions (different line styles). Kinetic energy (upper panel) shows more rapid fluctuations in the tracking condition (thick solid line), corresponding to the abrupt reaction of the manual tracking system to the 60° bends (Mrotek et al. 2005). However, the average KE was similar across the three conditions.

In Fig. 6d, we show the relation between nKE and path distance for the naïve subject who performed the experiment twice. As in the histograms, the tracking condition is represented with black symbols, the tracing condition is represented with white symbols, and the drawing condition is represented with gray symbols. Naturally, for this subject, and for all subjects, there was a strong positive relation between nKE and distance. However, contrary to the hypothesis of changes in arm configuration, neither the slope nor the intercept was significantly different across conditions. To combine the results across subjects, we evaluated each regression to predict nKE at a common distance (1.2 m, the overall

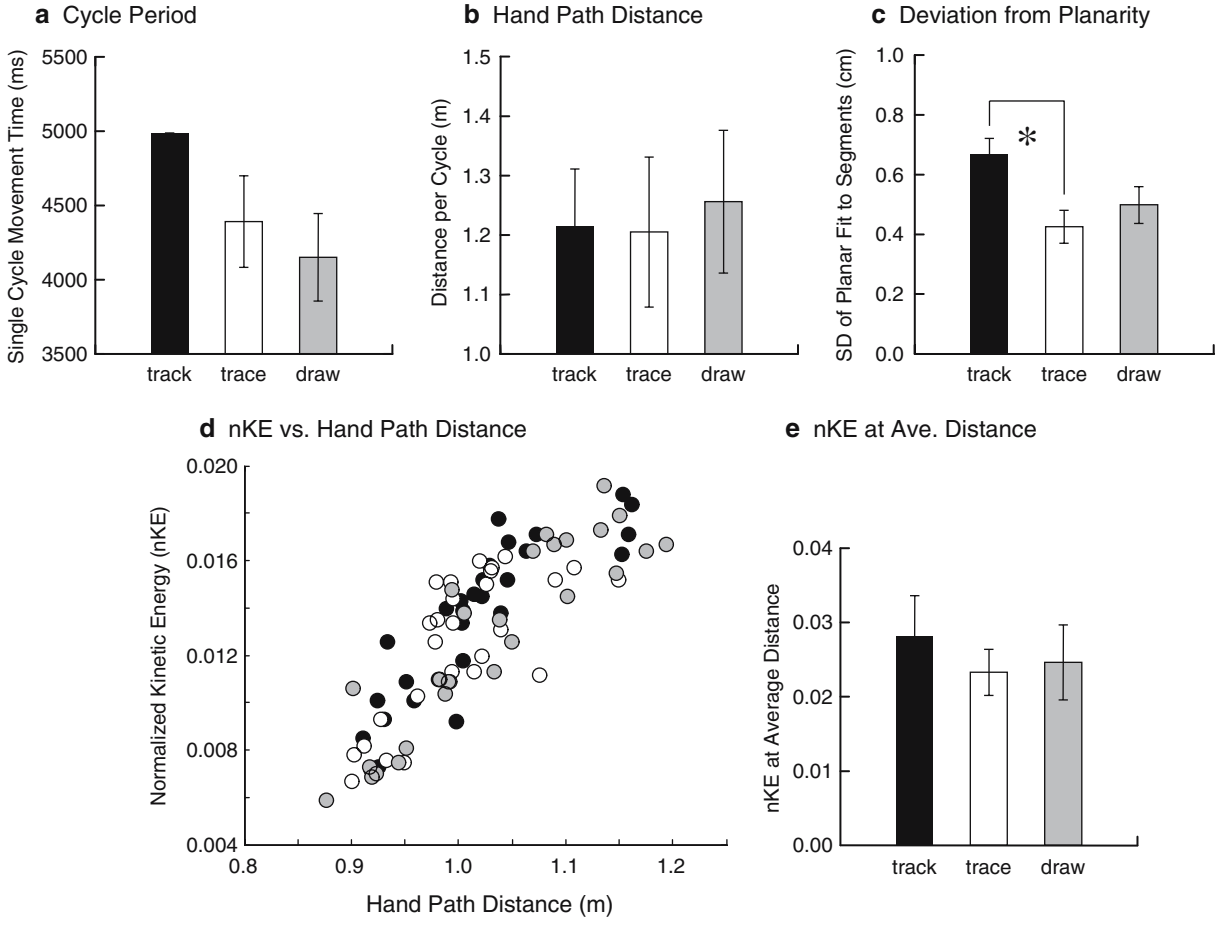

Fig. 6 Kinematic and kinetic parameters for the Cassini shapes. Panels *a*, *b* and *c* show, for all Cassini shapes, the grand mean ($n = 6$) and standard error (*SE*) of cycle period (**a**), hand path distance (for one cycle) (**b**), and deviation from planarity (for sub-cycles) (**c**). Panel **d** shows the relation between normalized kinetic energy (*nKE*) and hand path distance, for the naïve subject who performed the experiment twice (14 Cassini shapes × 2 repetitions = 28 data points for each condition). *Black*, *open*, and *gray* symbols refer to the tracking, tracing and drawing conditions, respectively. Panel **e** shows the grand mean (±SE) *nKE* at a distance of 1.2 m, for each of the conditions. ANOVA on $n = 6$ observations for each condition revealed a significant difference in only one case (*$P < 0.05$ in **c**)

average distance). As shown in Fig. 6e, using an ANOVA ($n = 6$ subjects), we found no difference across conditions, with nearly identical values for tracing and drawing.

Differences in the 2/3 power law across conditions

In the Methods section, we presented a simulation that will aid interpretation of deviations from the expected value of 0.33, for the slope of the linear fit of log velocity to log radius of hand path curvature (Fig. 5). This simulation showed that a value higher than 0.33 would correspond to a movement that was faster for a large radius of curvature (a relatively flat curve) and slower for a small radius of curvature (an indent or a bend), compared to a movement composed of sinusoids. Figure 7a shows that the Cassini shapes for the tracing condition came very close to the ideal value of 0.33. However, there were significant differences across conditions (Fig. 7a–c), as well as significant variation across sizes (Fig. 7b), sub-cycles (Fig. 7c) and shapes (Fig. 7d) within the tracing condition.

In Fig. 7a, we show a comparison of the equivalent Cassini shapes in the front and side orientations, as well as a comparison across conditions. Within each condition, we used a paired t-test to compare the front and side versions for each subject and each particular shape (i.e., no bend, 60° long axis bend, 30° long axis bend, 60° short axis bend, etc.). We found no significant differences within condition ($P > 0.05$), and thus the different mechanical parameters (i.e., inertia of the arm, joint angles) for the front and side orientations did not produce different exponents for the velocity/curvature relation. We also did t-tests across conditions (paired for subject, shape and orientation) and found that in each case, the tracing condition had a lower exponent than its tracking or drawing counterpart ($P < 0.001$). Furthermore, we did multiple one-sample t-tests to see whether the exponent values summarized in Fig. 7a were significanly different from 0.33. With the significance level adjusted for multiple comparisons ($0.05/6 = 0.008$), we

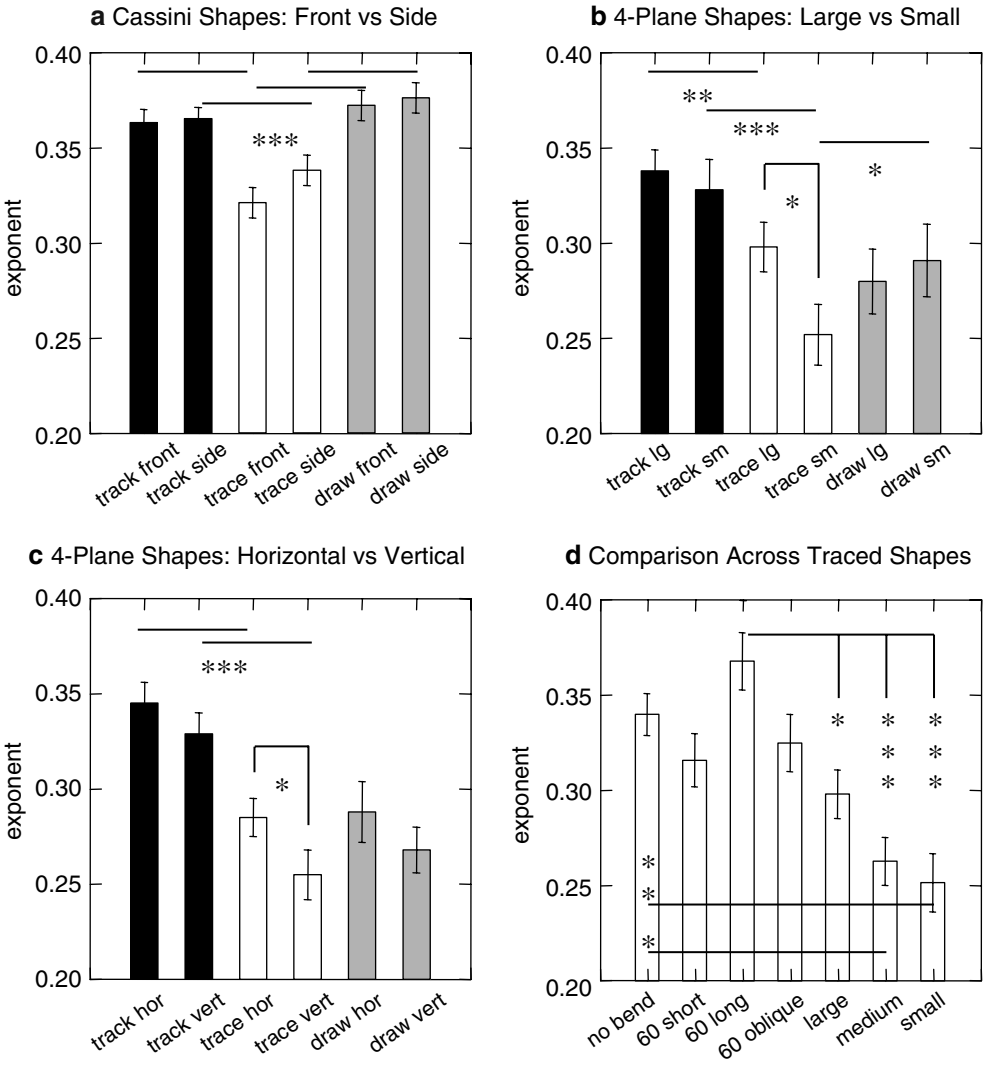

Fig. 7 Overview of the slope of the log velocity versus log radius plots for various conditions. Paired t-tests were used to compare front and side orientations of Cassini shapes (**a**), large (*lg*) and small (*sm*) sizes of 4-Plane shapes (**b**), and horizontal (*hor*) and vertical (*vert*) segments of 4-Plane shapes (**c**). We also used paired t-tests to compare across conditions: tracking (*black bars*), tracing (*white bars*) and drawing from memory (*gray bars*). We used an ANOVA (with $n = 48 = 8$ subcycles $\times$ 6 subjects) to compare seven of the main categories of shapes within the tracing condition (**d**). Significant differences are indicated as $^{*}P < 0.05$, $^{**}P < 0.01$, or $^{***}P < 0.001$

found that the track and draw conditions (front and side) had exponents that were different from 0.33. For the tracing of front Cassini shapes, the average value was 0.327 ($t = 0.322$, df = 167, $P = 0.748$); for the tracing of side Cassini shapes the average value was 0.333 ($t = 0.329$, df = 167, $P = 0.743$).

In a similar way, we compared the exponents for pairs of large and small 4-plane shapes. We found that the large shape had a significantly larger exponent than the small shape, but only for the tracing condition (0.30 vs. 0.25, $P < 0.05$). Although the target shape had constant curvature, many subjects flattened it into the frontal plane (see Fig. 3), thus producing tighter curves at the transitions between horizontal and vertical segments. The relatively small exponent for the small shape implies that, for a given range of curvature values, subjects tended to use a smaller range of velocity values. Indeed, for the small 4-plane shape shown in Fig. 3, the speed profile rarely came close to zero (compared to the profile shown in Fig. 4) and the exponent value for most cycles was less than 0.33 (as indicated above each sub-cycle in the speed profile). Using multiple one way *t*-tests, we found that two of the conditions illustrated in Fig. 7b had exponents that differed significantly from 0.33. These conditions were tracing small (mean = 0.252, $t = 5.052$, df = 47, $P < 0.001$) and drawing large (mean = 0.280, $t = 2.968$, df = 47, $P < 0.005$).

Figure 7b also shows differences in corresponding 4-plane shapes across conditions, and Fig. 7c shows differences in corresponding sub-cycles of 4-plane shapes across conditions. The main difference was the relatively high exponent for the tracking condition (black bars) compared to the tracing condition (white bars). The difference was the greatest when small tracked shapes were compared to small traced shapes (Fig. 7b, $P < 0.001$), and when the tracked vertical segments were compared to the traced vertical segments (Fig. 7c, $P < 0.001$).

Figure 7c also shows that only within the tracing condition, the vertical segments had significantly smaller exponents than the horizontal segments ($P < 0.05$). A representative example is provided in Fig. 3, where the horizontal segment shown in green (fifth segment) had an exponent of 0.34, while the next vertical segment (orange, sixth segment) had an exponent of 0.22. Since the exponent is the slope of a log velocity versus. log radius plot, it is difficult to appreciate the correspondence between the speed profile and the value of the exponent, without also taking into account the curvature. However, it is clear that a rapid fluctuation between maximum and minimum velocity, as occurs in the last two sub-cycles in Fig. 3, generally corresponds to larger values for the exponent. Regarding Fig. 3, it is also interesting to note that despite the constant velocity of the 4-plane tracking target, all subjects showed cyclic modulation of the speed profile. However the average range of maximum to minimum speeds was much smaller for the 4-plane shapes (0.2–0.6 m/s, 0.2–0.4 m/s and 0.1–0.3 m/s for the large, medium and small 4-plane shapes, respectively) than for the Cassini shapes (0.02–0.5 m/s).

One of the main goals of this analysis was to describe variations from the 2/3 power trajectory due to geometric parameters. Differences across large and small shapes (Fig. 7b) and across horizontal and vertical segments (Fig. 7c) might have been attributed to the different inertia of the arm for movements in different planes, or to different geometric relations between joint angles and position in work space. However, these differences were found only in the tracing condition and not when comparable shapes were drawn from memory. In fact, the difference between large and small shapes, while not statistically significant, had the opposite sign in the drawing condition (Fig. 7b). This suggests an interpretation based on planning to trace the visible shape, rather than the relation between joint angles and hand trajectory.

Thus, we focused our attention on the geometric properties of traced shapes; we used an ANOVA, to compare exponents across Cassini shapes (pooled front and side orientations) with the four types of 60° bend axis and also across the 4-Plane shapes (pooled horizontal and vertical segments) with the three sizes (Fig. 7d). Scheffé post hoc analysis revealed many significant differences across shapes. For example, as illustrated in Fig. 4, Cassini shapes with long axis bends were associated with the largest exponent values. The segment shown in blue (fourth segment) began with an indent at nearly zero velocity, which quickly increased to nearly maximum velocity during the relatively flat part of the shape. Thus, in general, a relatively large exponent means that the subject slowed down more than expected for the bends and indents and moved faster than expected along the relatively flat segments. Thus, in the tracing condition, the arm movement strategy varied according to features of the traced shape.

Discussion

We compared various aspects of tracking, tracing, and drawing and found that these behaviors were similar in terms of the size and shape of the hand path, the overall speed of the arm movement, and the arm configuration (i.e., the series of arm postures and the energy expenditure). Surprisingly, in spite of the overall similarities in the movements, we found subtle, but highly significant differences in the relation between hand path velocity and curvature. When compared with the tracing condition, in the tracking and drawing conditions subjects slowed down more around the bends, the indents and the transitions between horizontal and vertical planes; they also moved more quickly during the relatively flat parts of the path. In the two sections below, we will briefly discuss the similarities across conditions and then focus on the possible implications of the difference in the velocity/curvature relation.

Similarities in KE and planarity across conditions

During tracking, the cycle period (and thus the average tracking speed) was set by the target; it was 5 s for the Cassini shapes. During tracing and drawing, most subjects moved about 10% faster, and therefore we time-normalized (to 5 s) the two center cycles (cycles two and three), prior to subsequent analysis. There was also variability across subjects (but not across conditions for a given subject) in the overall size of the shapes (i.e., the hand path distance), and therefore, we took both speed and distance into account before using kinetic energy as a measure of changes in joint angle trajectories.

Normalized kinetic energy (nKE) has been shown to be a sensitive measure of small changes in arm geometry due to changes in movement strategy. For example, in a study of sequences of reaching movements, the nKE of the first movement differed depending upon which second movement was planned (Klein Breteler et al. 2003). This occurred in the absence of a difference in the hand path of the first movement. Also, simulation studies suggested that neuromuscular strategies for selecting initial and final arm configurations may take nKE into account (Soechting et al. 1995; Flanders et al. 2003; Klein Breteler et al. 2003). Thus, we chose this parameter to test the hypothesis that visually-guided and memory-guided movements are generated in a fundamentally different manner. Our results did not support this hypothesis. Instead, we found that arm geometry was very similar across visual-memory conditions.

There has been some debate about whether the tendency for the hand to move in a plane reflects mechanics, biologically coupled joint rotations, or higher-level visual–spatial representations (Sternad and Schaal 1999; Soechting and Terzuolo 1986; Pellizzer et al. 1992). Since the target shapes were piece-wise planar, it was expected that the deviation from planarity would be low in the tracing condition. If we had found that deviation from planarity was higher in the drawing condition, this would have argued against the hypothesis that the planarity arises from the visual–spatial representation of a complex 3D shape (presumably drawing from memory would be based upon this representation). However, somewhat unexpectedly, we found that hand paths were equally planar in the tracing and drawing conditions. Therefore, our results do not refute the hypothesis that planarity is a prominent aspect of the memory-based representation of 3D shapes.

Implications of deviations from the 2/3 power law

A common approach to investigate the underlying principles for the planning and execution of movements is to look for invariant features. One of the well-known invariant features is that the velocity profile for movements between two targets is bell-shaped, in line with the principle of minimization of jerk (Flash and Hogan 1985). For 2D and 3D movement trajectories, the 2/3 power law has also been widely reported and has been thought to be a fundamental constraint of the central nervous system in the formation of rhythmic curved trajectories (e.g., Wann et al. 1988).

In the past years, several studies have explored whether one of the two principles described above could be a consequence of the other. In particular, Todorov and Jordan (1998) claimed that minimum jerk could be a guiding principle to explain the velocity for curved trajectories in 3D space. These authors assumed that for a given path of the hand in space, the speed profile will be the one that minimizes jerk. Analysis of the mathematical relationship between this smoothness constraint and the 2/3 power law revealed that in both 2D and 3D, the power law is equivalent to setting the jerk along the normal to the path to zero. Their conclusion was that extending the 2/3 power law with a smoothness constraint gave a better fit to the experimental trajectories.

As mentioned in the introduction, the validity of the 2/3 power law as a fundamental mechanism in the formation of rhythmic trajectories was also questioned by Schaal and Sternad (2001) and by Richardson and Flash (2001). These studies revealed systematic violations of the 2/3 power law, in the sense that the exponent of the relation could deviate significantly from the theoretical value. In fact, Schaal and Sternad (2001) reported deviations of up to 40%. Moreover, these authors used an anthropomorphic robot, which generated end-point trajectories modeled as simple harmonic oscillations of robot joint angles. Their analysis of the endpoint trajectories revealed that the power law is systematically violated for larger trajectories. These authors concluded that subjects employed smooth oscillatory pattern generators in joint space to realize the required movement patterns and that the precise exponent of the non-linear relationship between tangential velocity and curvature depends on the geometric relation between joint angles and the position of the end-effector in the workspace.

A good comparison of the results of various studies is complicated by the fact that very few have investigated 3D movements in detail and that the paradigm used could be very different. In the studies by Richardson and Flash (2001) and Todorov and Jordan (1998), subjects were asked to move along complex visible trajectories in a 2D plane. In the study by Schaal and Sternad (2001), subjects were instructed to make cyclic movements in a horizontal or vertical plane, without a clear target trajectory. Thus, the goal of our study was to directly compare 3D movements across various visual-memory conditions.

We found that the 2/3 power law was followed most closely (i.e., with an exponent near 0.33) in the condition where the target path was fully visible. However, we also found that the tracing of the small 4-plane shape, but not the large 4-plane shape, was fit with an exponent that was significantly different from 0.33 (in contrast to the results of Schaal and Sternad 2001). Only in the tracing condition did we find an influence of size and spatial orientation on the value of the exponent. Within

the tracing condition, we also found a dramatic influence of the type of Cassini shape, with the long axis bend shapes having the highest value for the exponent. This may suggest an explanation based on the ability to plan ahead for the geometric features of the fully visible shape.

We did not find significantly different values for the exponents for frontal and side presentations of the Cassini shapes. Since the mechanical parameters of the arm (i.e., inertia, joint angles) are different for the frontal and side orientations, these results tend to argue against an effect of mechanical parameters on the exponent of the 2/3 power law. The observation that the exponents were significantly different for the tracing condition in comparison with the nearly identical movements in the tracking and drawing conditions also argues against an explanation based on geometric parameters, and in favour of other (strategic or cognitive) factors involved in the planning and/or execution of movements.

Similarities between tracking and drawing

Given the complexity of the 3D target paths, we did not expect the movements made from memory to be so similar to the movements made in the tracking and tracing conditions. Had we anticipated this, we could have used a delay time greater that 30 s, to see whether this introduced more distortion. It seems especially interesting that, in all of the parameters that we evaluated, the tracking condition was almost never significantly different from the drawing condition. This may suggest a common set of strategies for visual guidance (during tracking) and internal guidance (during drawing).

The target shapes in our study were designed to contain a range of curvature values, as well as abrupt bends, and planar segments. The bends and other local changes in the path (i.e., indents and horizontal-vertical transitions) were the key features that we used to break the hand path into sub-cycles. Unfortunately, we did not record eye movements during our experiment; it would have been interesting to see whether subjects made saccades to path bends and indents during the tracking condition. This type of strategy would be consistent with the results of studies of hand-eye coordination, where key task-related targets are fixated, apparently to aid in planning an arm movement sequence (Johansson et al. 2001; Flanagan and Johansson 2003). Furthermore, manual interception movements are correlated with fixation errors in a case where saccades (but not smooth pursuit) are misdirected due to the Duncker illusion (Soechting et al. 2001). Both these examples suggest that fixation locations are used to guide tasks involving arm movements.

We now speculate that eye fixations and/or prolonged manual dwell times in bends and indents may have guided the learning of the target shape in the tracking condition and the memory of that shape for the drawing condition. In our analysis, after breaking the hand path into sub-cycles based on bends and indents, we examined these sub-cycles to evaluate the velocity/curvature relation. Based on the results, it seems that subjects may have also made use of these key features to learn (during tracking) and remember (for drawing) the target trajectory. This would explain why subjects tended to spend more time in these bends and indents and less time in the relatively flat areas, during the tracking and drawing conditions. Thus, we propose that deviations from the 2/3 power law can reveal a subject's strategy for learning and recalling a complex trajectory.

Acknowledgements This work was supported by NIH grant R01 NS027484. We thank Brian Bergmark for his help with preliminary experiments.

References

Flanagan JR, Johansson RS (2003) Action plans used in action observation. Nature 424:769–771

Flanders M, Hondzinski JM, Soechting JF, Jackson JC (2003) Using arm configuration to learn the effects of gyroscopes and other devices. J Neurophysiol 89:450–459

Flash T, Hogan N (1985) The coordination of arm movements: an experimentally confirmed mathematical model. J Neurosci 5:1688–1703

Gnadt JW, Bracewell RM, Andersen RA (1991) Sensorimotor transformation during eye movements to remembered visual targets. Vision Res 31:693–715

Hollerbach JM (1980) An oscillation theory of handwriting. Biol Cybern 39:139–156

Johansson RS, Westling G, Backstrom A, Flanagan JR (2001) Eye-hand coordination in object manipulation. J Neurosci 21:6917–6932

Klein Breteler M, Hondzinski JM, Flanders M (2003) Drawing sequences of segments in 3D: Kinetic influences on arm configuration. J Neurophysiol 89:3253–3263

Lacquaniti F, Terzuolo C, Viviani P (1983) The law relating the kinematic and figural aspects of drawing movements. Acta Psychologica 54:115–130

Massey JT, Lurito JT, Pellizzer G, Georgopoulos AP (1992) Three-dimensional drawings in isometric conditions: relation between geometry and kinematics. Exp Brain Res 88:685–690

McIntyre J, Stratta F, Lacquaniti F (1997) Viewer-centered frame of reference for pointing to memorized targets in three-dimensional space. J Neurophysiol 78:1601–1618

McIntyre J, Stratta F, Lacquaniti F (1998) Short-term memory for reaching to visual targets: psychophysical evidence for body-centered reference frames. J Neurosci 18:8423–8435

Mrotek LA, Gielen CCAM, Flanders M (2005) Manual tracking in three dimensions. Exp Brain Res. DOI 10.1007/s00221-005-0282-9

Pellizzer G, Massey JT, Lurito JT, Georgopoulos AP (1992) Three-dimensional drawings in isometric conditions: planar segmentation of force trajectory. Exp Brain Res 92:326–337

Richardson MJE, Flash T (2001) Comparing smooth arm movements with the two-thirds power law and the related segmented-control hypothesis. J Neurosci 22:8201–8211

Schaal S, Sternad D (2001) Origins and violations of the 2/3 power law in rhythmic three-dimensional arm movements. Exp Brain Res 136:60–72

Soechting JF, Buneo CA, Herrmann U, Flanders M (1995) Moving effortlessly in three-dimensions: Does Donders' law apply to arm movement? J Neurosci 15:6271–6280

Soechting JF, Engel KC, Flanders M (2001) The Duncker illusion and eye-hand coordination. J Neurophysiol 85:843–854
Soechting JF, Tillery SIH, Flanders M (1990) Transformation from head- to shoulder-centered representation of target direction in arm movements. J Cogn Neurosci 2:32–43
Soechting JF, Terzuolo CA (1986) An algorithm for the generation of curvilinear wrist motion in an arbitrary plane in three-dimensional space. Neurosci 19:1393–1405
Soechting JF, Terzuolo CA (1987) Organization of arm movement in three-dimensional space. Wrist motion is segmented. Neurosci 23:53–61
Stoker JJ (1969) Differential geometry. Wiley, New York
Sternad D, Schaal S (1999) Segmentation of endpoint trajectories does not imply segmented control. Exp Brain Res 124:118–136
Todorov E, Jordan MI (1998) Smoothness maximization along a predefined path accurately predicts the speed profiles of complex arm movements. J Neurophysiol 80:696–714
Wann J, Nimmo-Smith I, Wing AM (1988) Relation between velocity and curvature in movement: equivalence and divergence between a power law and a minimum-jerk model. J Exp Psychol 14:622–637